Journal of Physics: Condensed Matter

Switching through symmetry breaking for transmission in a T-shaped photonic waveguide coupled with two identical nonlinear micro-cavities

IOP PUBLISHING JOURNAL OF PHYSICS: CONDENSED MATTER

J. Phys.: Condens. Matter **23** (2011) 315303 (6pp) doi:10.1088/0953-8984/23/31/315303

Switching through symmetry breaking for transmission in a T-shaped photonic waveguide coupled with two identical nonlinear micro-cavities

Evgeny Bulgakov[1,2] **and Almas Sadreev**[1]

[1] Kirensky Institute of Physics, 660036, Krasnoyarsk, Russia
[2] Siberian State Aerospace University, Krasnoyarsk Rabochii, 31, Krasnoyarsk, Russia

E-mail: almas@tnp.krasn.ru

Received 21 April 2011, in final form 27 June 2011
Published 19 July 2011
Online at stacks.iop.org/JPhysCM/23/315303

Abstract
Using coupled mode theory we consider transmission in a T-shaped waveguide coupled with two identical symmetrically positioned nonlinear micro-cavities with mirror symmetry. For input power injected into the central waveguide we show the existence of a symmetry breaking solution which is a result of mixing of the symmetrical input wave with an antisymmetric standing wave in the Fabry–Pérot interferometer. With growth of the input power, a feature in the form of loops arises in the solution which originates from bistability in the transmission in the output left/right waveguide coupled with the first/second nonlinear cavity. The domains of stability of the solution are found. The breaking of mirror symmetry gives rise to nonsymmetrical left and right outputs. We demonstrate that this phenomenon can be explored for all-optical switching of light transmission from the left output waveguide to the right one by application of input pulses.

(Some figures in this article are in colour only in the electronic version)

1. Introduction

It is believed that future integrated photonic circuits for ultrafast all-optical signal processing require different types of nonlinear functional elements such as switches, memory and logic devices. Therefore, both the physics and designs of such all-optical devices have attracted significant research efforts during the last two decades, and most of these studies utilize the concepts of optical switching and bistability. One of the simplest bistable optical devices which can be built up in photonic integrated circuits is a single micro-cavity coupled with an optical waveguide or waveguides [1]. Its transmission properties depend on the intensity of incident light when the cavity is filled with a Kerr nonlinear material. If the characteristic optical wavelength much exceeds the size of the nonlinear cavity, it can be presented by a single isolated mode coupled with the waveguide.

For an extension of the number of nonlinear cavities, say two, coupled with the photonic crystal (PhC) waveguide, one can expect, at first sight, two bistable resonances as was indeed obtained in [2–5]. However, the effects of self-induced variation of resonance properties and mutual interference of the nonlinear cavities could give rise to a much richer variety of resonance phenomena. The situation crucially depends on the architecture and symmetry of the system. If the coupled cavities are different, both eigenmodes, bonding and antibonding are coupled with the waveguide between the cavities. However, for the nonlinear cavities the coupling with the antibonding mode might turn to zero in a self-consistent way. This results in hidden eigenmodes, bound states in continuum (BSC). Nevertheless the lack of the superposition principle in the nonlinear system gives rise to excitation of the BSC by transmitting light over the waveguide. This results in resonances of a rather peculiar butterfly shape [6, 7].

The case of two identical nonlinear cavities coupled symmetrically with the single waveguide is especially interesting by symmetry breaking with growth of input power. This phenomenon is developed in nonlinear optics [8–12] with the establishment of one or more asymmetric states which no longer preserve the symmetry properties of the original state.

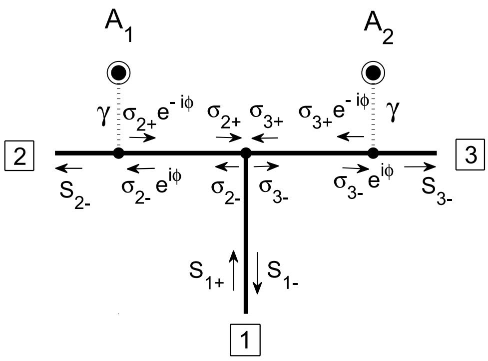

Figure 1. A schematic T-shaped waveguide coupled with two identical nonlinear optical cavities shown by filled bold circles. The cavities are coupled with output waveguides 2 and 3 via the constant γ shown by dotted lines. The input wave amplitude labeled as $S_{1+} = E_{\text{in}}e^{-i\omega t}$ is applied through waveguide 1.

In particular Maes *et al* [13, 14] considered symmetry breaking for the cavities aligned along the waveguide, i.e. the Fabry–Pérot architecture close to the system considered in [10]. This system is symmetric relative to the inversion of the transport axis if equal power is injected on both sides of the coupled cavities. The case of the cavities aligned perpendicular to the waveguide was considered in [15, 16]. The symmetry breaking was found also for the case of many coupled nonlinear optical cavities in a ring-like architecture [17, 18]. It is worth noting that the phenomenon of the symmetry breaking is well established also in two nonlinear fiber couplers [19–21]. The Schrödinger lattice with two or more nonlinear sites is an adequate model of these optical systems [22].

Maes *et al* [13] also proposed a switching device that employs a symmetry breaking bifurcation. Because of the symmetry there are always two equivalent asymmetric states: one where the left output power is larger than the right output power, and the mirrored state, where the right output is larger than the left output. By increasing or decreasing one of the inputs, it is possible to switch between these two states. Thus, this scheme provides the option of switching with positive pulses, which is not obvious in single-cavity devices. In the present paper we explore that approach for the T-shaped waveguide coupled with two identical nonlinear micro-cavities, as shown in figure 1. The input light power can provoke symmetry breaking to result in different outputs in the terminals 2 and 3. Sharply changing the light incident on waveguide 1 we demonstrate all-optical switching between left and right outputs.

2. Coupled mode equations

We consider a light given by the amplitude S_{1+} incident on the waveguide 1 and outputs into all three terminals, as shown schematically in figure 1. The outgoing amplitudes are labeled as S_{1-}, S_{2-} and S_{3-}. Each nonlinear optical cavity is assumed to be given by single mode amplitudes $A_j, j = 1, 2$ and coupled with the photonic crystal waveguides 2, 3 via the coupling constant γ shown in figure 1 by dotted lines. For simplicity, in the present paper we neglect the direct coupling of the cavities and the couplings of the cavities with the input waveguide 1.

We describe the process of the light transmission and excitation of optical cavity modes using the coupled mode theory (CMT). This approach was presented by Snyder for propagation in nonuniform media, where the modes are those associated with both the discrete and continuous eigenvalue spectrum [23, 24]. We note that the idea of separation of total Hilbert space into the discrete and continuous states with further projection of the total space onto the subspace of discrete states was first raised by Livsic [25] and independently by Feshbach [26] to formulate the concept of a non-Hermitian effective Hamiltonian in the quantum theory of scattering. For the present system we use the CMT formulated in [27, 28]:

$$\begin{aligned} i\dot{A}_1 &= (\omega_1 - i\gamma)A_1 + i\sqrt{\gamma}\sigma_{2-}e^{i\phi} \\ i\dot{A}_2 &= (\omega_2 - i\gamma)A_2 + i\sqrt{\gamma}\sigma_{3-}e^{i\phi} \end{aligned} \tag{1}$$

where the eigenfrequencies of the nonlinear optical cavities are shifted because of the Kerr effect

$$\omega_j = \omega_0 + \lambda|A_j|^2, \quad j = 1, 2. \tag{2}$$

The phase ϕ as shown in figure 1 is the optical length through which light goes between the T-junction and the cavities. These CMT equations are to be complemented by the equations for light amplitudes at each cavity

$$\begin{aligned} S_{2-} &= \sigma_{2-}e^{i\phi} - \sqrt{\gamma}A_1, \\ S_{3-} &= \sigma_{3-}e^{i\phi} - \sqrt{\gamma}A_2, \\ \sigma_{2+}e^{-i\phi} &= -\sqrt{\gamma}A_1, \\ \sigma_{3+}e^{-i\phi} &= -\sqrt{\gamma}A_2. \end{aligned} \tag{3}$$

The T-connection connects ingoing and outgoing amplitudes by the S-matrix as follows

$$\begin{pmatrix} S_{1-} \\ \sigma_{2-} \\ \sigma_{3-} \end{pmatrix} = \begin{pmatrix} a & c & c \\ b & d & e \\ b & e & d \end{pmatrix} \begin{pmatrix} S_{1+} \\ \sigma_{2+} \\ \sigma_{3+} \end{pmatrix}. \tag{4}$$

In particular, if we follow the continuity and Kirchhoff equations we obtain $a = d = -1/3, b = c = e = 2/3$. Equations (1), (3) and (4) form a full system of equations for nine amplitudes $A_1, A_2, \sigma_{2+}, \sigma_{2-}, \sigma_{3+}, \sigma_{3-}, S_{1-}, S_{2-}, S_{3-}$.

After simple algebra we obtain the following equations

$$\left(i\frac{\partial}{\partial t} - H_{\text{eff}}\right)\begin{pmatrix} A_1 \\ A_2 \end{pmatrix} = \frac{2i}{3}\sqrt{\gamma}e^{i\phi}S_{1+}(t)\begin{pmatrix} 1 \\ 1 \end{pmatrix}, \tag{5}$$

where we take that the incident amplitude $S_{1+} = E_{\text{in}}e^{-i\omega t}$ and

$$H_{\text{eff}} = \begin{pmatrix} \omega_1 - i\gamma(1 - \frac{1}{3}e^{2i\phi}) & -\frac{2}{3}i\gamma e^{2i\phi} \\ -\frac{2}{3}i\gamma e^{2i\phi} & \omega_2 - i\gamma(1 - \frac{1}{3}e^{2i\phi}) \end{pmatrix}. \tag{6}$$

For the sake of simplicity we take for the optical length [7, 14]

$$\phi = \omega - \omega_c. \tag{7}$$

The solution of the stationary CMT equation (5) for $A_j(t) = A_je^{-i\omega t}$ and $S_{1+}(t) = E_{\text{in}}e^{-i\omega t}$ is given by the inverse of the matrix $\omega - H_{\mathrm{eff}}$, whose matrix elements in turn depend on this solution via equation (2). A numerical self-consistent procedure of the solution gives us the frequency behavior of the light intensities presented in figure 2(a) for the small input amplitude $E_{\mathrm{in}} = 0.05$. There are, at least, three branches for small E_{in}. The first one shown by a solid gray line preserves the mirror symmetry. Thereby this state shows the same feature as the single nonlinear cavity coupled with the waveguide, i.e. resonance enhancement of the light intensities with further bistability if we increase the input power. This feature is not seen in figure 2(a) but is clearly seen in figures 4(a) and (b) for larger input amplitude. The other two branches break the mirror symmetry and are related by the symmetry transformation $I_1 \leftrightarrow I_2$ where $I_j = |A_j|^2$. One of these branches shown in figure 2(a) by solid (I_1) and dashed (I_2) lines has the form of closed curves which limit the points marked by stars for $E_{\mathrm{in}} \to 0$. These points define the BSC which for the present case of the T-shaped structure are standing waves between two off-channel cavities. As shown in [6, 7, 30], the BSC exists for the special case of singular matrix $\omega - H_{\mathrm{eff}}(\omega)$. The condition for the BSC is formulated as follows

$$\det[\omega - H_{\mathrm{eff}}(\omega)] = 0. \tag{8}$$

It is easy to see that it happens if the following equation is fulfilled

$$\mathrm{e}^{2\mathrm{i}\phi} = 1, \qquad \phi = \pi m, \tag{9}$$

where m is the integer. This quantization condition differs from the condition for the Fabry–Pérot system [7, 29] $\phi = \pi m/2$. This difference is due to the waveguide 1 being connected with the T-shaped system at the middle as shown in figure 1. Therefore only that state is trapped between three waveguides which has nodal points at all connections shown in figure 1 by bold points. From the first condition for the BSC $\omega = \omega_0 + \lambda I_j$ and equation (7) we instantly obtain the BSC frequencies and intensities

$$\begin{gathered} \omega_b = \omega_c + \pi m, \qquad A_1 = -A_2, \\ I_j = (\omega_c - \omega_0 + \pi m)/\lambda. \end{gathered} \tag{10}$$

Substituting the parameters given in figure 2 one can find that the positions of BSCs marked by a star are exactly described by these simple equations.

If the system were linear, light incident on waveguide 1 would excite both cavities symmetrically $A_1 = A_2$, while the antisymmetric BSC localized between the cavities would exist independently of the input light [30]. However, in the nonlinear system there is no principle of linear superposition. This results in mixing of the transport symmetrical solution with the antisymmetric BSC [6, 7, 15] to give rise to the mirror symmetry breaking. In what follows we define that mechanism of symmetry breaking as symmetric and antisymmetric mixing (SAM). Thus, as soon as $E_{\mathrm{in}} \neq 0$ the BSC becomes a quasi-bound state. The solution for the intensities acquires a specific shape of closed curves for each intensity, as shown in figure 2(a). These closed curves are reflected in the transmission resonance of a peculiar shape of butterfly as shown in figure 2(b) obtained first in [7]. For the aim of all-optical switching the phenomenon of the symmetry breaking

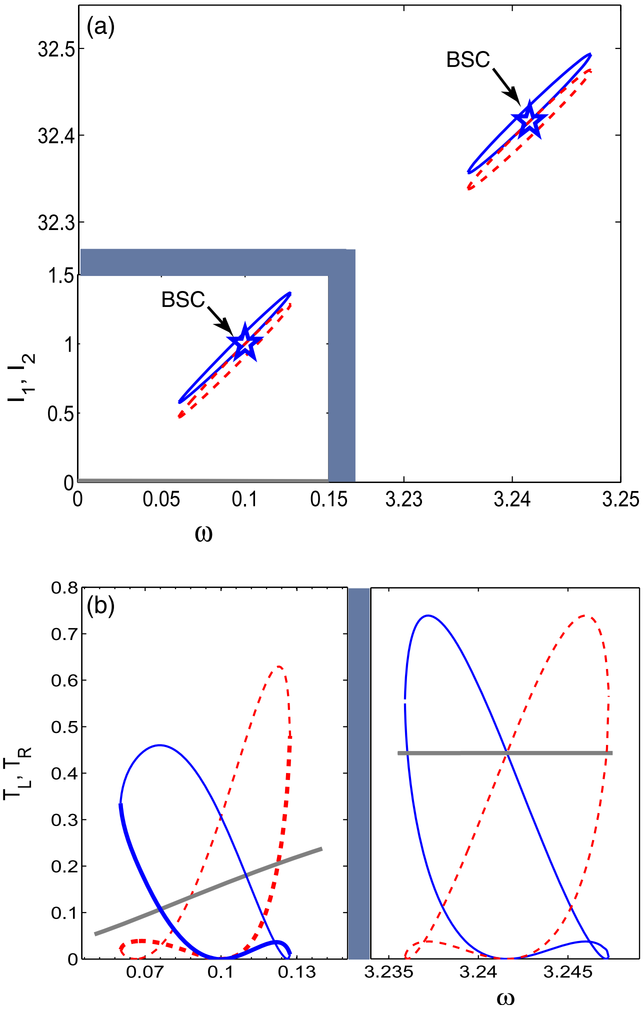

Figure 2. The frequency behavior of (a) light intensities $I_1 = |A_1|^2$ (solid blue line) and $I_2 = |A_2|^2$ (dashed red line), and (b) the transmissions T_L (solid blue line) and T_R (dashed red line) from the input waveguide 1 into the output ones 2 and 3, respectively, for $E_{\mathrm{in}} = 0.05$. The stability domain of the branch is marked by a thick line. The symmetry preserving state is shown by a gray solid line. The parameters of the CMT model are $\omega_c = 0.1$, $\omega_0 = 0$, $\gamma = 1$, $\lambda = 0.1$. The BSC points given by equation (10) are marked by stars. Gray filled areas skip from the first BSC to the second one.

solution is the most important. Correspondingly we obtain that the outputs in the left and right waveguides are not equal. The symmetry breaking branches localized around the BSC point shown by stars in figure 2 exist at any $E_{\mathrm{in}} \neq 0$ and, therefore, the phenomenon has no threshold in the input power. However, the stability is restricted by the input power and crucially depends on the frequency ω_c. These SAM symmetry breaking solutions are shown in figures 2–4. Figure 3 demonstrates the SAM solution evolving for $\omega_c \to 0$. The stability was studied by standard methods given, for example, in the [31, 32] with details given in [15].

As we increase ω_c, the domain of stability of these SAM solutions is shrinking. However, as we increase the input amplitude ($E_{\mathrm{in}} > 0.64$ for $\omega_c = 0.75$), a feature in the form of a loop arises in the symmetry breaking solution, as shown

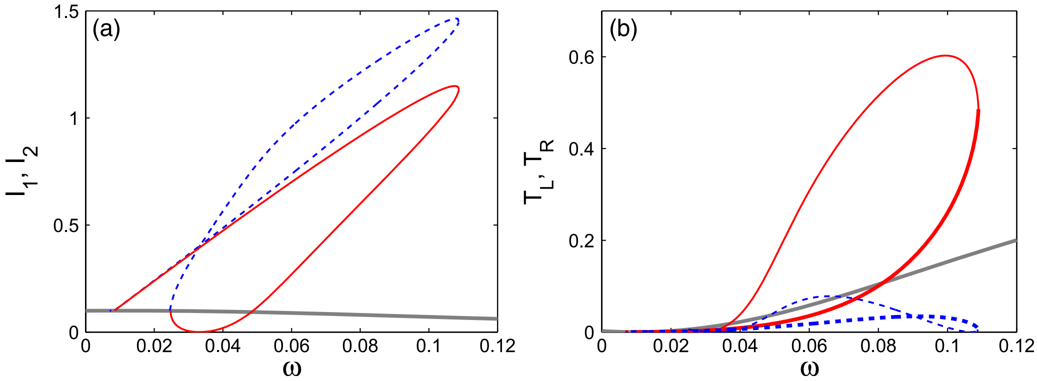

Figure 3. The same as in figure 2 but for $\omega_c = 0$, $E_{\rm in} = 0.2$.

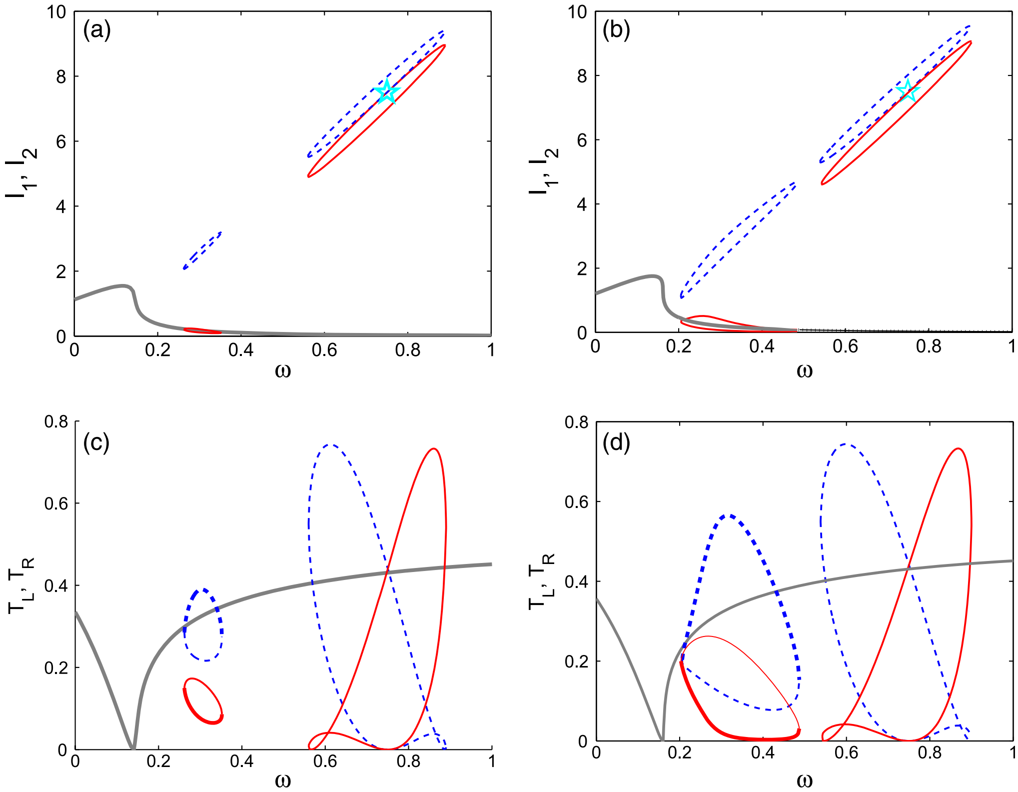

Figure 4. The frequency behavior of light intensities (a) and the output transmissions T_L and T_R for $E_{\rm in} = 0.65$, and (b) and (d) for the stronger input amplitude $E_{\rm in} = 0.7$. The parameters of the CMT model are $\omega_c = 0.75$, $\omega_0 = 0$, $\gamma = 1$, $\lambda = 0.1$. The intensity of the first/second cavity is shown by a dashed/solid line. Correspondingly the left/right output transmissions are shown by dashed/solid lines. Domains of stability are distinguished by the thickness of lines. The gray line corresponds to the symmetry preserving solution which is stable.

in figure 4(a). The loop feature in the intensities is reflected in the output transmission in the form of loops too as shown in figure 4(c). With further growth of the input amplitude $E_{\rm in}$ the loops are expanded providing almost complete blocking of the output into the right waveguide, as shown in figures 4(b) and (d). There is a symmetrically equivalent branch which blocks the output into the left waveguide. The loops are the result of bistable transmission through the left/right output waveguide coupled with the first/second nonlinear cavity. Assume $I_1 \gg I_2$, so we can neglect nonlinearity in the second cavity. Then the approximate solution of equation (5) is

$$\begin{aligned} A_1 &\approx \{f[\omega-\omega_0+{\rm i}\gamma(1-{\rm e}^{2{\rm i}\phi(w)})]\} \\ &\quad\times \{[(\omega-\omega_0-\lambda|A_1|^2)(\omega-\omega_0+{\rm i}\gamma(1-{\rm e}^{2{\rm i}\phi(w)})) \\ &\quad+ 4\gamma^2{\rm e}^{4{\rm i}\phi(\omega)}/9]\}^{-1} \\ A_2 &\approx \{f[\omega-\omega_0-\lambda|A_1|^2+{\rm i}\gamma(1-{\rm e}^{2{\rm i}\phi(w)})]\} \\ &\quad\times \{[(\omega-\omega_0-\lambda|A_1|^2)(\omega-\omega_0+{\rm i}\gamma(1-{\rm e}^{2{\rm i}\phi(w)})) \\ &\quad+ 4\gamma^2{\rm e}^{4{\rm i}\phi(\omega)}/9]\}^{-1}, \end{aligned} \tag{11}$$

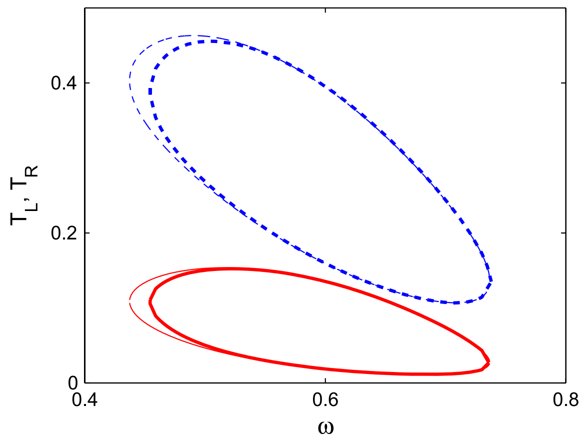

Figure 5. The transmissions to the left and right waveguides calculated by use of exact equations (5) (thick line) and by use of approximated equations (11) (thin lines) for $\omega_c = 1$, $E_{\text{in}} = 0.88$.

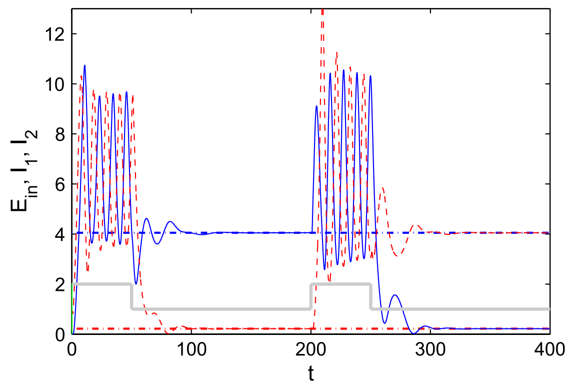

Figure 7. The time dependence of the light amplitudes $|A_1|$, $|A_2|$ in the cavities (solid and dashed respectively) which follow the impulses of the input amplitude E_{in} (gray). We take the cavities as oscillating in a nonsymmetric way: $A_1 = 0$, $A_2 = 1$.

where $f = 2\mathrm{i}\sqrt{\gamma}\mathrm{e}^{\mathrm{i}\phi(\omega)}/3$. One can see that because of the nonlinearity of the first equation in equation (11) a bistability might occur for the first cavity mode A_1. Then the second cavity mode A_2 simply follows A_1 through the second equation in equation (11). In figure 5 we show the transmission calculated approximately with the use of equation (11) (thin line). Comparison with the solution of exact equations (5) (thick line) demonstrates good agreement. This, indeed, shows that the additional features of the loop type in the symmetry breaking solution are related to the individual bistabilities of the transmission in the separate structure segment waveguide 2 or 3 with the corresponding nonlinear cavity 1 or 2. The solutions crucially depend also on the frequency position of the BSC ω_c, as shown in figure 3.

Figure 6 demonstrates that the symmetry breaking solution is dependent on the input amplitude E_{in}. One can see that there is a domain in E_{in} where the transmission to the left output waveguide is almost fully suppressed for a given branch. For the second mirrored branch the transmission to the right waveguide is suppressed. This result is extremely important for the switching of the output power from the left waveguide to the right one. In order to switch the system from one asymmetric state to the other we follow [13, 17] and apply pulses of the input power injected into the waveguide 1. The direct numerical solution of the temporal CMT equation (5) with $S_{1+}(t) = E_{\text{in}}(t)\mathrm{e}^{-\mathrm{i}\omega t}$ is shown in figure 7 which demonstrates the switching effect. The stepwise time behavior of amplitude $E_{\text{in}}(t)$ is shown by a gray line. One can see that after the first impulse of the input amplitude the oscillations of the cavity amplitude relax onto the stable stationary solutions with broken symmetry. Moreover after each next impulse the state of the system transmits from one asymmetric state to the other as was observed by Maes *et al* [13].

3. Conclusions

We extended the phenomenon of symmetry breaking in the T-shaped photonic crystal waveguide coupled with two identical nonlinear cavities using the coupled mode theory. The phenomenon had already been established in the Fabry–Pérot interferometer architecture for cavities aligned along the waveguide [10, 13, 14] and in the architecture of the cavities aligned perpendicular to the waveguide [15, 16]. In the present T-shaped waveguide we find that the symmetry breaking originates from the antisymmetric BSC which is

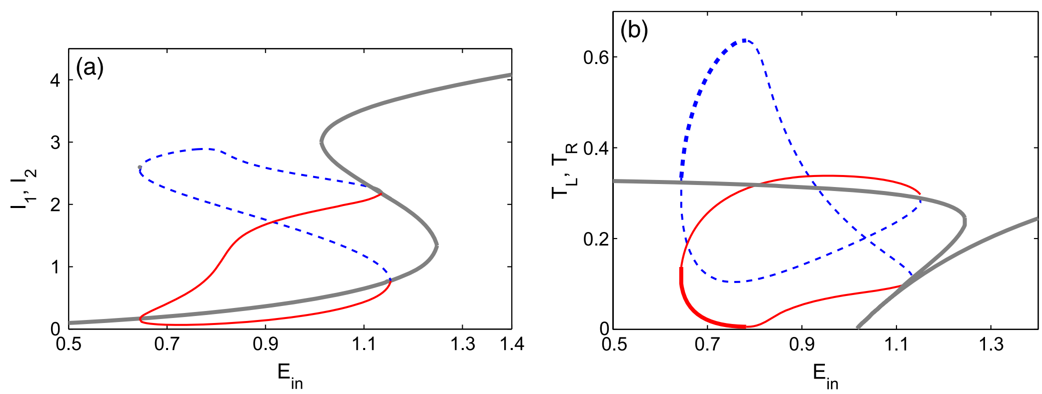

Figure 6. (a) The light intensities at the cavities and (b) the transmissions T_L (dashed) and T_R (solid) versus the input amplitude E_{in} for $\omega = 0.3$, $\omega_c = 0.75$, $\lambda = 0.1$, $\gamma = 0.1$. The domain of stability is emphasized by thick lines in (b).

trapped between three waveguides. Because of the lack of the principle of linear superposition in the nonlinear system the antisymmetric BSC couples with the symmetric transport solution. As a result the solution breaks the symmetry. This SAM mechanism has no threshold in the light power incident on the input waveguide. However, the domain of stability of the symmetry breaking state crucially depends on the optical length ω_c of the light path from the T-connection to the micro-cavities.

With growth of the input power the symmetry breaking is expected to be strong. Then the light intensity in the first cavity might be weak while the second cavity can be excited to be so strong that the optical bistability occurs for separate transmission in the right output waveguide. This results in loops in the transmission onto the right waveguide. Equivalently this consideration is applied to the left waveguide coupled with the first nonlinear cavity too. The left/right light output might be almost blocked, which is the most important property of the symmetry breaking branches for the all-optical switching of outputs in the T-shaped waveguide. We demonstrated the switching mechanism based on the symmetry breaking solutions in the T-shaped waveguide coupled with two nonlinear cavities. This phenomenon gives a method of almost perfect all-optical switching of output light from waveguide 2 to waveguide 3 by application of a sharp change of the input light intensity. This process is shown in figure 7.

References

[1] Joannopoulos J, Johnson S G, Winn J N and Meade R D 2008 *Photonic Crystals: Molding the Flow of Light* (Princeton, NY: Princeton University Press)
[2] McGurn A R 2003 *Chaos* **13** 754
[3] McGurn A R 2004 *J. Phys.: Condens. Matter* **16** S5243
[4] Miroshnichenko A E, Kivshar Yu, Etrich C, Pertsch T, Iliew R and Lederer F 2009 *Phys. Rev.* A **79** 013809
[5] Miroshnichenko A E 2009 *Phys. Rev.* E **79** 026611
[6] Bulgakov E N and Sadreev A F 2009 *Phys. Rev.* B **80** 115308
[7] Bulgakov E N and Sadreev A F 2010 *Phys. Rev.* B **81** 115128
[8] Haelterman M and Mandel P 1990 *Opt. Lett.* **15** 1412
[9] Peschel T, Peschel U and Lederer F 1994 *Phys. Rev.* A **50** 5153
[10] Babushkin I V, Logvin Yu A and Loĭko N A 1998 *Quantum Electron.* **28** 104
[11] Torres J P, Boyce J and Chiao R Y 1999 *Phys. Rev. Lett.* **83** 4293
[12] Longchambon L, Treps N, Coudreau T, Laurat J and Fabre C 2005 *Opt. Lett.* **30** 284
[13] Maes B, Soljačić M, Joannopoulos J D, Bienstman P, Baets R, Gorza S-P and Haelterman M 2006 *Opt. Express* **14** 10678
[14] Maes B, Bienstman P and Baets R 2008 *Opt. Express* **16** 3069
[15] Bulgakov E N, Pichugin K N and Sadreev A F 2011 *Phys. Rev.* B **83** 045109
[16] Bulgakov E N, Pichugin K N and Sadreev A F 2011 *J. Phys.: Condens. Matter* **23** 065304
[17] Otsuka K and Ikeda K 1987 *Opt. Lett.* **12** 599
[18] Huybrechts K, Morthier G and Maes B 2010 *J. Opt. Soc. Am.* B **27** 708
[19] Akhmediev N and Ankiewicz A 1993 *Phys. Rev. Lett.* **70** 2395
[20] Tasgal R and Malomed B A 1999 *Phys. Scr.* **60** 418
[21] Gubeskys A and Malomed B A 2004 *Eur. Phys. J.* D **28** 283
[22] Brazhnyi V A and Malomed B A 2011 *Phys. Rev.* A **83** 053844
[23] Snyder A W 1970 *IEEE Microw. Theor. Technol.* **18** 383
[24] Snyder A W 1972 *J. Opt. Soc. Am.* **62** 1267
[25] Livsic M S 1957 *Sov. Phys.—JETP* **4** 91
[26] Feshbach H 1958 *Ann. Phys. (NY)* **5** 357
Feshbach H 1962 *Ann. Phys. (NY)* **19** 287
[27] Fan S, Suh W and Joannopoulos J D 2003 *J. Opt. Soc. Am.* A **20** 569
[28] Suh W, Wang Z and Fan S 2004 *IEEE J. Quantum Electron.* **40** 1511
[29] Fan S, Villeneuve P R, Joannopoulos J D, Khan M J, Manolatou C and Haus H A 1999 *Phys. Rev.* B **59** 15882
[30] Bulgakov E N, Pichugin K N, Sadreev A F and Rotter I 2006 *JETP Lett.* **84** 430
[31] Litchinitser N M, McKinstrie C J, deSterke C M and Agrawal G P 2001 *J. Opt. Soc. Am.* B **18** 45
[32] Cowan A R and Young J F 2003 *Phys. Rev.* E **68** 046606